Tellus (1992), *44A*, 414–424

A model of the deep water flow into the Baltic Sea

By LARS GIDHAGEN* and BERTIL HÅKANSSON, *The Swedish Meteorological and Hydrological Institute, S-601 76 Norrköping, Sweden*

(Manuscript received 14 November 1989; in final form 22 June 1992)

ABSTRACT

Deep water renewal in the Baltic basins is a consequence of gravitationally driven bottom currents, transporting water from the North Sea area towards the deeper parts of the estuary. The dense currents have to pass several topographic constrictions, one of them being the Bornholm Channel. In this study, a numerical two-layer, limited area model has been applied to the southern Baltic Proper, in which the Bornholm Channel is located. The mathematical problem was solved as an initial value problem with rigid boundaries. The results were used to obtain a simplified formula, determining the dense bottom water flow as a function of the stratification in the upstream Arkona Basin. This relation makes it possible to calculate the deep water inflow in detail, since hydrographic observations are frequent, whereas direct transport measurements are scarce in the area. The calculated flow characteristics in the Bornholm Channel are in accordance with observations. The volume flow was found to vary between 0.9×10^4 and 2.9×10^4 m^3 s^{-1}, using upstream basin values of density differences and pycnocline depths close to the observed mean magnitudes. The model indicates that inertia, Coriolis and frictional forces along with the upstream stratification and topography control the channel flow. Quasi-steady state is obtained within 24 h, whereas the time-scale for a water volume to pass the channel is approximately 2.3 days.

1. Introduction

Gravitationally driven bottom currents have a great impact on the transport of properties within the sea. For example salinity, temperature and oxygen may change considerably in the deeper layers due to these currents. Dense bottom currents exist in many basins which exchange water with surrounding areas, such as the Mediterranean outflow, the flow through the Denmark Strait and the Faroe-Shetland Channel. Also the deep water in the Black and Baltic Seas are renewed by dense inflowing water from the Mediterranean and the North Sea, respectively. Although several physical factors (as density, topography, friction, rotation and mixing) may influence the flow characteristics, estimates of the flow often rely on the assumption of a dynamic control at the constriction. This implies that the flow rate can be determined from the upstream conditions. For narrow sounds the flow might be controlled in the same way as a dam spilling water over a barrier (cf. Whitham, 1974), whereas in wider sounds the Coriolis force will influence the transport capacity. Models based on hydraulic controls at topographic constrictions has been investigated by Whitehead et al. (1974) and Gill (1977), using a rectangular cross section in the channel and by Borenäs and Lundberg (1988) with a parabolic cross section. For relatively long constrictions, friction may also be important as a controlling factor of the flow (cf. Pratt, 1986). In these models, the flow rate is uniquely determined by the upstream stratification and the topography of the channel. This state of affairs simplifies the estimation of volume flow and transport of substances, since hydrographic conditions in upstream basins are known in many cases (for example, there exists a large amount of observations on the hydrographic state of the Baltic Sea, discussed, among others, by Fonselius (1967) and Matthäus (1984) & (1985)). Similar transport

* Present affiliation is Indic, P.O. Box 1514, S-600 45 Norrköping, Sweden.

models have been applied for quantitative estimates of the Baltic Sea bottom water renewal, although the assumption of control sections within the Baltic Sea has still not been verified by measurements.

The Baltic and the North Sea are connected through narrow and shallow sounds, the Belt Sea and the Öresund with sill depths of 18 and 8 meters, respectively (Fig. 1). The main inflow takes place through the Belt Sea (Jacobsen, 1980), whereas 1/3 of the volume flow passes through the Öresund. In the Baltic, the inflowing water first enters the Arkona Basin, from where the dense water flows to deeper parts of the Baltic Sea through the Bornholm Channel. This is a gently sloping and narrow transition between the Arkona and the Bornholm Basin. Observational evidence of the inflowing dense water is mainly coming from measurements made in this channel (cf. Petrén and Walin (1976) and Walin (1981)).

Some modelling efforts of the dense bottom current in the Baltic Sea have been made. Pedersen (1977) assumed a dense bottom current balanced by frictional forces and mixing, flowing along a gently sloping flat bottom. Lundberg (1983) investigated a diagnostic model with a frictional coupling between the down- and cross-stream pressure gradients, applied to the Bornholm Channel. Stigebrandt (1987) used hydrographic observations in the Arkona Basin to determine the geostrophic flow rate and its associated salt transport. His basic assumption is that the inflow is more stationary and unidirectional in the Bornholm Channel than in the Belt Sea and Öresund, the latter currents being mainly barotropic and strongly oscillatory. As no sill appears to exist between the Arkona Basin and the Bornholm Channel, Stigebrandt suggested that there should be a deep water pool in the Arkona Basin, leaking water into the Bornholm Channel. The magnitude of this flow was determined by integrating Margules formula and assuming maximum volume flow rate. Further use of this approach to calculate the deep water flow between the sub-basins in the Baltic has been undertaken by Omstedt (1987, 1989), modelling the hydrography and especially the thermal regime of the Baltic Sea.

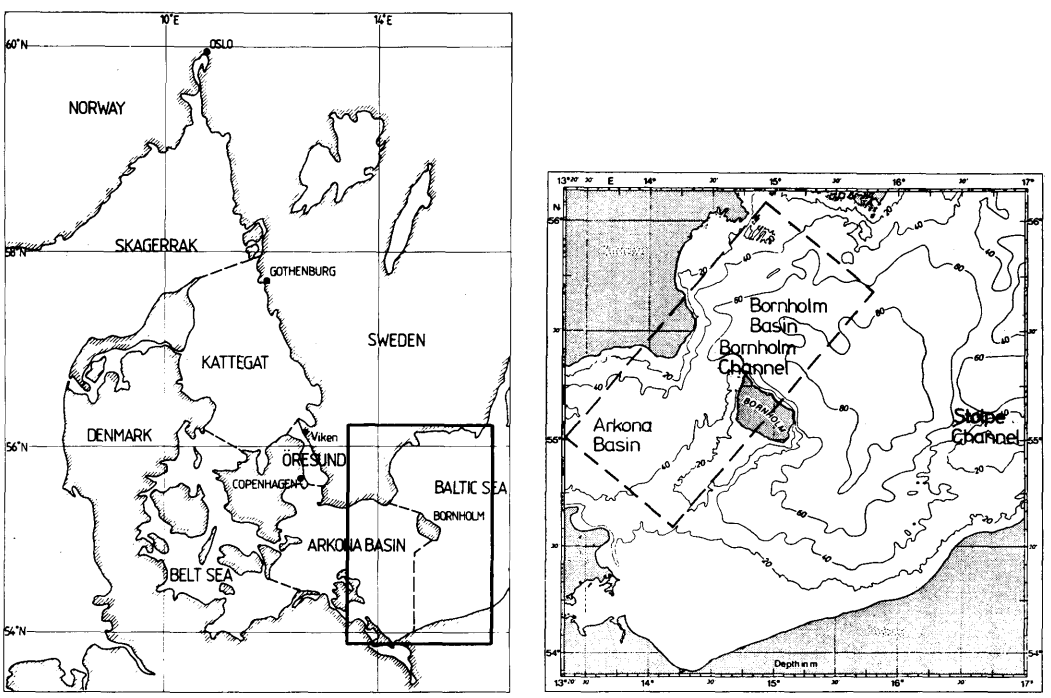

Fig. 1. Overview and bathymetric chart of the Bornholm Channel.

The present study is an attempt to briefly summarize the physical characteristics of the flow through the Bornholm Channel and to calculate the deep water volume flux using a two-layer model. The time evolution of the water exchange between the Arkona and Bornholm Basin is calculated, taking into account the topographic features of the area in a simplified way. In the parameter regime governing the dynamics in the Bornholm Channel, the model demonstrates a considerable influence of bottom friction, Coriolis force and stratification on the transport capacity.

The following section briefly summarizes the bottom current characteristics in the Bornholm Channel and its typical balance of forces. Section 3 describes the numerical model and the geometrical configuration. The results are presented and discussed in Section 4, followed by conclusions in Section 5.

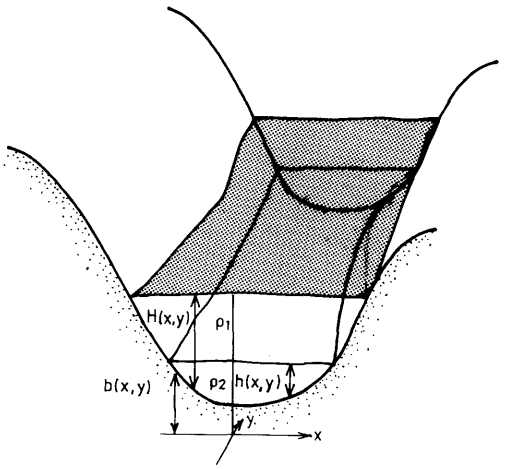

Fig. 2. Illustration and nomenclature of the two-layer stratified channel.

2. Flow characteristics in the Bornholm Channel

A scaling analysis is used to define the overall characteristics of the deep water flow in the Bornholm Channel. The analysis is based on the reduced-gravity shallow water equations over an inclined bed. The equations governing the evolution in time of the flow are:

$$\frac{\partial u}{\partial t}+u\frac{\partial u}{\partial x}+v\frac{\partial u}{\partial y}-fv = -g'\frac{\partial h}{\partial x}-g'\frac{\partial b}{\partial x}-C_d\frac{u|u|}{h}, \quad (1)$$

$$\frac{\partial v}{\partial t}+u\frac{\partial v}{\partial x}+v\frac{\partial v}{\partial y}+fu = -g'\frac{\partial h}{\partial y}-g'\frac{\partial b}{\partial y}-C_d\frac{v|v|}{h}, \quad (2)$$

$$\frac{\partial h}{\partial t}+\frac{\partial uh}{\partial x}+\frac{\partial vh}{\partial y}=0. \quad (3)$$

Here u is the cross- and v the along-channel velocity component (cf. Fig. 2), f is the Coriolis parameter, $g'=g\,\Delta\rho/\rho_2$ is the reduced gravity, h is the bottom layer thickness, b is bottom elevation above a reference level and C_d is the drag coefficient used in the quadratic bottom friction term.

The magnitude of the scales and the dependent variables are listed in Table 1. Length, width and slope ($\theta\approx-\partial b/\partial y$) values are estimated from the Bornholm Channel bathymetry chart. The magnitudes of the along-channel velocity and the thickness of the bottom current were found from the measurements presented by Petrén and Walin (1976), whereas the typical magnitude of the upstream stratification (i.e., the salinity distribution) was taken from Matthäus (1985). Applying his salinity data to the two-layer model suggests that a salinity difference of 6 Psu is appropriate. How to choose a representative value of the bottom drag coefficient C_d is more intricate. The reference velocity should normally be taken at 1 m above the bottom, but in a layered model the available velocity is the one which has been vertically integrated in each layer. Since the layer in this

Table 1. *Characteristics of the Bornholm Channel*

Length (L)	6.0×10^{4} m	reduced gravity (g')	4.7×10^{-2} m s^{-2}
Width (B)	1.0×10^{4} m	Coriolis parameter (f)	1.2×10^{-4} s^{-1}
Thickness (h)	1.0×10^{1} m	slope (θ)	4.0×10^{-4}
Velocity (V)	3.0×10^{-1} m s^{-1}		

case may be 10–15 m thick, the drag coefficient should probably be slightly lower than if applied to the depth at 1 m. A value close to 2.0×10^{-3} is frequently choosen (Csanady, 1982), but field measurements from shelf regions show higher values, $C_d = 3.0 \times 10^{-3} - 11.0 \times 10^{-3}$ (Chriss and Caldwell, 1982 and Grant et al., 1984). The magnitude of 3.0×10^{-3} was taken to be a reasonable estimate in the present investigation (a test with a lower value is discussed in Section 4).

The order of magnitude estimates of the flow parameters in the Bornholm Channel are used in the scaling analysis of the governing equations. It follows from the continuity equation that the cross-channel velocity becomes $U \approx B/LV$, where B and L are the cross- and along-channel width, respectively. Inserting this result in the cross-flow momentum equation and introducing the scales according to Table 1 (after division with V^2/B), the following non-dimensional numbers and magnitudes are obtained:

$$fB^2/VfTL \quad B^2/L^2 \quad B^2/L^2 \quad fB/V \quad g'h/V^2 \quad C_d B^3/hL^2$$
$$(0.03) \quad (0.03) \quad (4) \quad (5.2) \quad (0.09)$$

After a few inertial periods ($fT > 1$) the flow is mainly geostrophic, since $fT \gg fB^2/VL$ when $fB/V \sim O(1)$ and $B/L \sim O(10^{-1})$. The same scaling for eq. (2) (and division with V^2/L) yields:

$$L/VT \quad 1 \quad 1 \quad fB/V \quad g'h/V^2 \quad g'\theta L/V^2 \quad C_d L/h$$
$$(1) \quad (1) \quad (4) \quad (5.2) \quad (13) \quad (18)$$

The along-channel adjustment time may be estimated from the characteristics given in Table 1. In this case it will take $L/V \sim 2$ days for the dense water volume to reach the lower end of the channel. On the other hand, the scaling of the local time derivative gives quasi-stationary flow at any cross-section after a time period $T \gg T_f$ ($T_f = h/C_d V$). Here T_f is the frictional adjustment time, which is of the order of 3 h. The remaining 4 terms may be compared with the advection term using the following non-dimensional numbers:

$F^2 = V^2/g'h = 0.19$	Froude number.
$\mathrm{Ro} = V/fB = 0.25$	Rossby number.
$F_\theta^2 = V^2/g'\theta L = 0.08$	Froude number based on bottom slope.
$R = h/C_d L = 0.06$	Equivalent Reynolds number (Pingree and Maddock, 1980).

Since all non-dimensional numbers are less than one, advection is likely to be of minor importance in the channel. The main balance is between the forcing bottom slope and the retarding bottom friction, although advection, rotation and internal pressure forces are not small enough to be negligable.

3. The mathematical model

The bottom current is treated as a layer of constant density beneath a less dense layer. A rather novel two-phase technique is applied, in which the two water masses are treated as two different phases. The exchange of mass and momentum between the two phases can be fully controlled. With the restriction of no exchange of mass between the phases, it is appropriate to speak of two layers instead of two phases. The interface between the layers may move both horizontally and vertically, allowing it to intersect either the bottom or the surface of the fluid. The two-phase technique has earlier beeen tested and verified against analytical solutions of some well-known oceanic circulation problems (i.e., Funkquist et al., 1987).

The following simplifications are introduced in the present investigation: (i) no exchange of salt, mass and momentum between the layers; (ii) the density is constant within each layer; (iii) the hydrostatic pressure assumption is valid. The governing equations which follow from these simplifications are:

$$\frac{\partial}{\partial t} r_1 \rho_1 u_1 + \frac{\partial}{\partial x} r_1 \rho_1 u_1^2 + \frac{\partial}{\partial y} r_1 \rho_1 u_1 v_1$$
$$= -r_1 \frac{\partial p}{\partial x} + r_1 \rho_1 v_1 f - \delta$$
$$\times \frac{C_d \rho_1}{H} u_1 |u_1|, \tag{4}$$

$$\frac{\partial}{\partial t} r_2 \rho_2 u_2 + \frac{\partial}{\partial x} r_2 \rho_2 u_2^2 + \frac{\partial}{\partial y} r_2 \rho_2 u_2 v_2$$
$$= -r_2 \frac{\partial p}{\partial x} + r_2 \rho_2 v_2 f - r_2 g(\rho_2 - \rho_1)$$
$$\times \frac{\partial \xi_2}{\partial x} - \frac{C_d \rho_2}{H} u_2 |u_2|, \tag{5}$$

$$\frac{\partial}{\partial t} r_1 \rho_1 v_1 + \frac{\partial}{\partial x} r_1 \rho_1 u_1 v_1 + \frac{\partial}{\partial y} r_1 \rho_1 v_1^2$$

$$= -r_1 \frac{\partial p}{\partial y} - r_1 \rho_1 u_1 f - \delta$$

$$\times \frac{C_d \rho_1}{H} v_1 |v_1|, \tag{6}$$

$$\frac{\partial}{\partial t} r_2 \rho_2 v_2 + \frac{\partial}{\partial x} r_2 \rho_2 u_2 v_2 + \frac{\partial}{\partial y} r_2 \rho_2 v_2^2$$

$$= -r_2 \frac{\partial p}{\partial y} - r_2 \rho_2 u_2 f - r_2 g(\rho_2 - \rho_1)$$

$$\times \frac{\partial \xi_2}{\partial y} - \frac{C_d \rho_2}{H} v_2 |v_2|, \tag{7}$$

$$\frac{\partial}{\partial t} r_1 \rho_1 + \frac{\partial}{\partial x} u_1 r_1 \rho_1 + \frac{\partial}{\partial y} v_1 r_1 \rho_1 = 0, \tag{8}$$

$$\frac{\partial}{\partial t} r_2 \rho_2 + \frac{\partial}{\partial x} u_2 r_2 \rho_2 + \frac{\partial}{\partial y} v_2 r_2 \rho_2 = 0, \tag{9}$$

$$r_1 + r_2 = 1. \tag{10}$$

Here subscripts $_{1,2}$ denote the upper and lower layers respectively, $r_{1,2}$ is the volume fraction of the layer that occupies a grid cell. The eq. (4) to (10) are identical to the layered model equations (of which eqs. (1) to (3) are one example), noting that $r_1 = (H-h)H^{-1}$ and $r_2 = hH^{-1}$. u and v are the velocities in the x- and y-directions (more properly velocity resolutes, because a non-cartesian grid is used), and ξ_2 is the displacement of the interface. The terms in eqs. (5) and (6) containing ξ_2 express the baroclinic pressure gradients associated with the tilt of the interface and they are one of the primary forcing terms for the bottom current. H and h are the total and the bottom layer thickness, respectively. The bottom friction is parameterized with a quadratic bottom friction law, with C_d being the drag coefficient. The coefficient δ is used to decouple the top layer friction where a bottom layer is present. Hence, δ is equal to zero at places where the bottom layer thickness exceeds one meter and is equal to one otherwise. The calculations of the frictionless cases are technically performed by lowering the bottom drag coefficient two orders of magnitude ($C_d = 3.0 \times 10^{-5}$). The internal friction between the two layers is equal to zero for all cases considered here.

The numerically calculated solution is obtained by integrating eqs. (4) to (10) over finite domains or control volumes (cf. Spalding, 1981, 1985 and Spalding and Markatos, 1983). The interpolation schemes are fully implicit and upwind. The solution is iterative, starting with guessed values of a barotropic pressure common to both layers. The different layer velocities are then calculated over the complete region, taking into accout the baroclinic pressure term. The continuity error is lowered by pressure corrections added to the old pressure field. This will lead to velocity corrections and a new and smaller continuity error. In practice the shorter the time step, the fewer iteration steps (sweeps) are necessary in order to achieve convergence. The time step used in the deep water inflow calculations was 450 s for the frictional cases and 225 s for the frictionless cases. In all cases, 15 sweeps per time step were carried out.

Bodyfitted coordinates (BFC) are used in all three directions to allow for a good resolution of the channel geometry. Fig. 3 illustrates the horizontal view of the grid. In this case a coarse grid is obtained within the basins (with a typical spacing of approximately 1 to 5 and 9 km in the

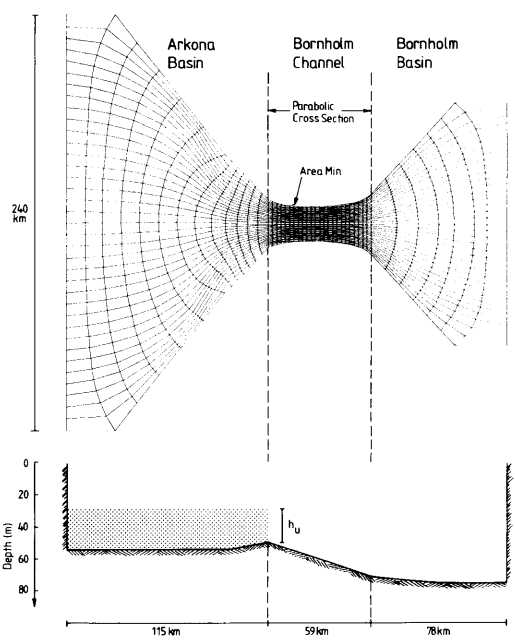

Fig. 3. Numerical grid and initial position of the dense bottom water.

cross- and along-channel directions, respectively), whereas the spacing within the channel is indeed more narrow (typical 0.6 and 2.4 km in the corresponding directions). The Rossby radius of deformation is close to 6 km, according to the data given in Table 1. Hence, the model grid is able to resolve mesoscale features in the channel, whereas this is only partly true in the two basins. Nevertheless, the body fitted coordinates make the cross-shore grid resolution dense enough so that coastal boundary flows are expected to be found in the solution. In the vertical direction the body fitted coordinates implies that each cell corner depth is set according to local topography.

The geometry of the Bornholm Channel is taken to be of constant slope and with a variable parabolic cross section (Fig. 3). Hence, the channel depth $H(x, y)$ is given by:

$$H(x, y) = H_o(y) + \beta(y)\, x^2, \tag{11}$$

$$H_o(y) = 45 + 4.0 \times 10^{-4} y, \tag{12}$$

$$\beta(y) = -6.0 \times 10^{-7} + 4.1 \times 10^{-16}(y - 37000)^2, \tag{13}$$

where $7400 \leqslant y \leqslant 66600$ m.

The governing equations were integrated over a closed volume without sources and sinks of mass and momentum, in order to avoid influence of open boundary conditions. The channel flow evolution was studied as an initial value problem with a distribution of the two water masses as shown in Fig. 3. The upstream basin was initially filled with dense bottom water to a level of ten or twenty meters above the sill depth, whereas the rest of the volume was occupied by less dense water. All velocities were set to zero. With these initial conditions the channel flow may be treated as an adjustment process similar to the classical rotational lock-exchange problem (i.e., Gill, 1976).

4. Results and discussions

The model simulations have been performed with three objectives in mind. The first concerns the relative importance of different processes for the transport capacity, whereas the second is to compare the results with field data from the Bornholm Channel and the Arkona Basin. The third objective is to derive a simplified transport formula relating the volume flow to the upper basin stratification. These objectives are discussed in the following subsections.

Table 2. *Basic parameters used in the model during the different runs*

Run	ΔS (psu)	g' (m s^{-2})	h_u (m)	f (s^{-1})	C_d
1a	10	0.0774	20	1.2×10^{-4}	3.0×10^{-3}
1b	10	0.0774	10	1.2×10^{-4}	3.0×10^{-3}
2a	6	0.0467	20	1.2×10^{-4}	3.0×10^{-3}
2b	6	0.0467	10	1.2×10^{-4}	3.0×10^{-3}
2c	6	0.0467	20	0.0×10^{-4}	3.0×10^{-3}
2d	6	0.0467	20	0.0×10^{-4}	0.03×10^{-3}
2e	6	0.0467	20	1.2×10^{-4}	0.03×10^{-3}
2f	6	0.0467	20	1.2×10^{-4}	1.5×10^{-3}
3a	2	0.0156	20	1.2×10^{-4}	3.0×10^{-3}
3b	2	0.0156	10	1.2×10^{-4}	3.0×10^{-3}

4.1. *Characteristics of the flow based on results from the model*

The aim of this subsection is to demonstrate the response of the model under different balances of forces and to examine the sensitivity of the model to the magnitude of the frictional drag coefficient, since this is the only parameter not uniquely determined. In the first case, the Coriolis force and the bottom friction was neglected in the model (Table 2, run 2d). The time evolution of the volume flow is illustrated in Fig. 4. After 48 h, the transport rate is still slowly increasing and no steady state has been achieved. In the second case the Coriolis force (Table 2 and Fig. 4; run 2e) is taken into account in the model. The volume flow is reduced approximately 50% compared to the first case, and the time to reach quasi-stationary flow in the channel is close to 24 h. A somewhat stronger reduction in volume flow is experienced in

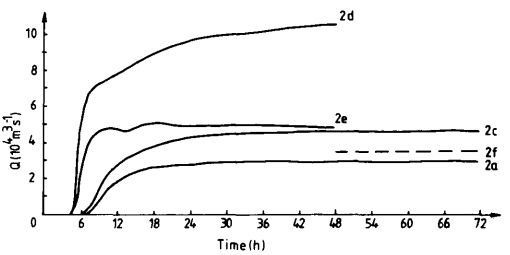

Fig. 4. Time evolution of transports at the section of smallest area (run 2a, c–f).

the third case when the bottom friction is included but the Coriolis force is neglected (Table 2 and Fig. 4; run 2c). The result obtained by combining rotation and friction shows that the volume flow rate is further reduced (Table 2 and Fig. 4; run 2a). These results as well as the scaling analysis of Section 2 demonstrate that the bottom current in the Bornholm Channel is indeed sensitive to both rotational and frictional effects, as both of them strongly influence the transport capacity. Note, also that the calculated flow rate is quasi-steady after about 2 inertial periods, as was shown to be the case in the scaling analysis made in Section 2.

In order to evaluate how sensitive the transport capacity is to changes in the magnitude of the bottom drag coefficient, the value of $C_d = 1.5 \times 10^{-3}$ instead of 3.0×10^{-3} was used in the third case as defined above (Table 2 and Fig. 4; run 2f). The numerical calculation show an increase of 20% in the transport capacity. Hence, the exact value of the drag coefficient seems to be essential when a detailed comparison with observations is to be made, but of less importance for an order of magnitude estimate. Still it might be argued that the quadratic drag formula may be too simple to give a realistic parameterization of the bottom friction. It is, however, beyond the scope of the present study to test other schemes of bottom friction parameterization.

Fig. 5 give another perspective of the bottom current behaviour for the cases above. For example, the Coriolis force reduces the cross-sectional area rather than lower the velocities, according to Figs. 5a and b. The frictional forces reduce the velocity in the channel from approximately 1.0 to 0.3 m s^{-1} (compare Figs. 5a with 5c). Hence, the combined effect of rotation and friction in the channel is to reduce both the velocity and the cross-sectional area of the bottom current. Note also that the reduced area results in a smaller mean depth, which contributes to an even stronger frictional effect as compared to the case without the Coriolis force. This tendency is seen in the magnitudes of the bottom layer velocity shown in Figs. 5d and c.

The case with a salinity difference of 6 Psu and an upstream pycnocline height $h_u = 20$ m (Table 2, run 2a) is used to illustrate the qualitative behaviour of the dense bottom current within the channel and the circulation induced in the upper and lower basins. Fig. 6a shows the depth contours

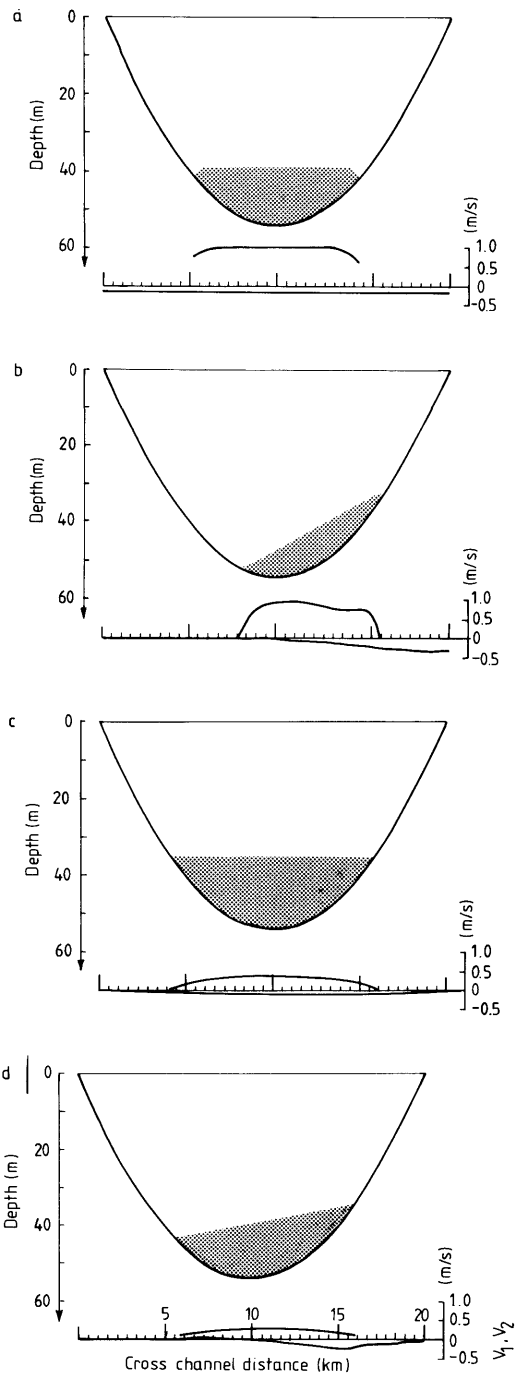

Fig. 5. Pycnocline position and velocity distribution within the two layers at the section of smallest area: (a) run 2d, (b) run 2e, (c) run 2c, (d) run 2a.

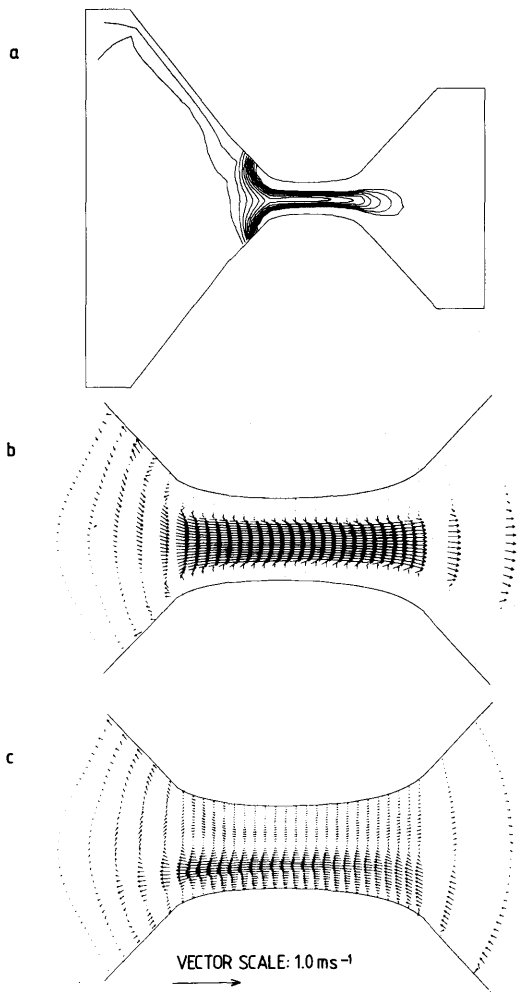

Fig. 6. Numerical results with $g' = 0.0467\ \mathrm{m\ s^{-2}}$ and $h_u = 20$ m: (a) bottom layer thickness (isoline spacing is 2 m); (b) bottom layer currents (only channel part is shown); (c) upper layer currents (only channel part is shown).

of the bottom layer after an inflow period of 3 days. The front of the dense bottom current has started to spread out into the downstream basin. Within the channel, the flow has come to a quasi-steady state which slowly changes as the upstream pool of bottom water is depleted. The bottom current originates as a coastal boundary flow along the northern side of the upstream basin (Fig. 6a) and continuous downstream mainly aligned along the southern boundary in the channel. This distribution of the flow is indeed similar to the result obtained by Gill (1976), who considered the time evolution of the adjustment process in a wide rectangular channel by removing a vertical obstruction.

Fig. 6b shows the velocity distribution within the bottom current, as it enters and passes the sloping channel. Asymmetries in the circulation due to the earth's rotation can be seen in the upstream and downstream basin. However, the top layer flow (Fig. 6c) is strongly asymmetrical also in the channel, with the highest velocities found on the southern side directed into the upper basin. On the northern side of the channel a weak counter-directed current is advancing towards the lower basin. Hence, in the upper layer a recirculation takes place, of which the cross-channel averaged volume flow should balance the lower layer flow for continuity reasons (since the total mass flow in both layers should vanish during quasi-steady conditions).

4.2. Comparison with observations

The second objective regards the possibility of the model to simulate the flow in the channel in comparison with the observations, using realistic stratifications in the upstream basin. However, there are no simultaneous observations on the upstream stratification and the velocity and salinity distribution in the Bornholm Channel. The comparison is therefore based on mean properties, since these are better known. The volume flow rate as well as the other characteristics of the flow determined by the model are taken during the quasi-steady state. The measured mean volume flow of the bottom current in the Bornholm Channel during the period from June 1973 to December 1974 was found to be $1.4 \times 10^4\ \mathrm{m^3\ s^{-1}}$ (cf. Walin, 1981). This flow rate covers the salinity range of 8 to 18.5 Psu. The mean salinity of this inflow slightly exceeds 13 Psu. The corresponding density difference (if temperature is considered unimportant) and, hence, the reduced gravity, are close to the magnitudes used in the model. The mean depth of the 13 Psu isohaline in the Arkona Basin is approximately 40 m, whereas during rare occasions this isohaline can reach a depth of 22 m according to Matthäus (1984). The depth of the upper basin (Arkona basin) at the entrance to the Bornholm Channel is 48 m. The upstream bottom layer thickness used in the model are 10 and 20 m

($h_u = 10$ and $h_u = 20$ m). The corresponding upper layer depth is thus 38 and 28 m, which are in close agreement with the observations given above. Hence, it is expected that the model results should reasonably agree with the observations in the Bornholm Channel. In those cases were the reduced gravity is 4.67×10^{-2} m s^{-2} and the bottom layer depth in the upper basin is 10 or 20 m the corresponding volume flow is 0.9×10^4 and 2.9×10^4 m^3 s^{-1}, which is in the right order of magnitude as observed by Walin (1981). Also the typical velocity of the dense current appears to agree with observations. The velocities during well-pronounced inflows are typically of the order 0.2 to 0.5 m s^{-1} according to Walin (1981), compared to 0.3 m s^{-1} as obtained by the model (cf. Fig. 5d). From this figure, the pycnocline tilt is estimated to 0.9×10^{-3}, which appear to be comparable with the measurements obtained by Petrén and Walin (1976), although it varied considerably during their observation period. At most the pycnocline tilt reached 1.5×10^{-3}.

4.3. *Some remarks on the transport rate in the Bornholm Channel*

The present analysis has shown that both rotation and friction are of importance for the flow in the Bornholm Channel. All calculations performed with these two terms included are summarized in Table 3, containing the initial data and the quasi-steady volume flow. The mean volume flow estimated from current and hydrographic measurements (cf. Walin, 1981) fall within the range given in Table 3. A particular aim of this study was to deduce a generalized formula for the transport rate, based on upstream values of pycnocline height (h_u) and density difference (g') solely. For that purpose, the following dependent non-dimensional transport rate is defined:

$$y = Qf/g'h_u^2. \tag{14}$$

The corresponding independent variable is obtained by taking the product of the rotational Froude number and the quotient of the typical bottom slope and the frictional bottom drag coefficient, yielding:

$$x = (\theta/C_d)(f^2B^2/g'h_u). \tag{15}$$

The characteristic magnitudes of the upstream conditions together with the site-specific topographical information were put into this non-dimensional parameter. By plotting these in a log-log diagram (Fig. 7) the best fit to a straight line shows that the following relation is obtained:

$$y = 0.3x^{0.28}. \tag{16}$$

Note, that the calculation with the lower bottom drag coefficient also fits this relation.

Stigebrandt (1987) and Omstedt (1987) have assumed the flow between the Arkona and Bornholm basin to be in geostrophic balance. The flow leaks out into the Bornholm Channel through a rectangular cross section. The transport rate of such a flow was found by Whitehead et al. (1974) (taking into account conservation of potential

Table 3. *Data on the initial state used in the model and the corresponding quasi-steady volume flow. The typical width (B) is 1×10^4 m and slope (θ) is 4×10^{-4} of the Bornholm Channel and the Coriolis parameter (f) is 1.2×10^{-4} s^{-1}*

Run	g' (m s^{-2})	h_u (m)	C_d	Q (m^3 s^{-1})
1a	0.0774	20	0.0030	4.2×10^4
1b	0.0774	10	0.0030	1.2×10^4
2a	0.0467	20	0.0030	2.9×10^4
2b	0.0467	10	0.0030	0.9×10^4
2f	0.0467	20	0.0015	3.5×10^4
3a	0.0156	20	0.0030	1.3×10^4
3b	0.0156	10	0.0030	0.4×10^4

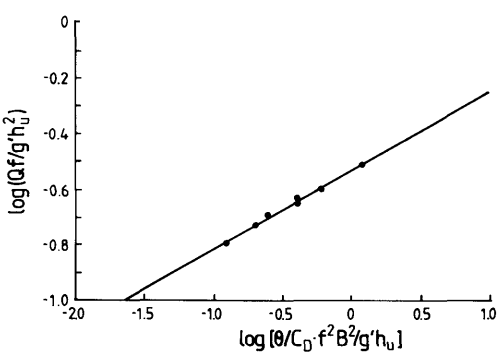

Fig. 7. Log-log scatter plot of the non-dimensional volume flow and the rotational Froude number including the ratio of channel slope and drag coefficient, see text for further information. Linear regression suggests that $y = 0.28x - 0.54$ with a correlation coefficient of $r^2 = 0.994$.

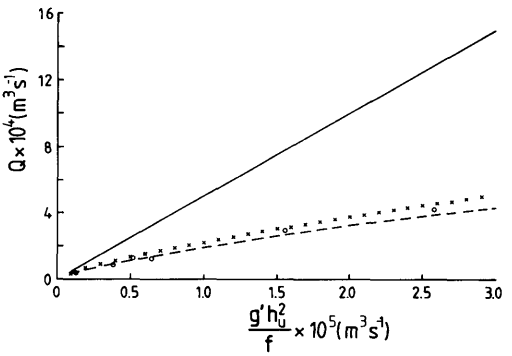

Fig. 8. Plot of the volume flow estimated from the purely geostrophic flow (−) and from eq. (18) with $h_u = 10$ m (− −) and $h_u = 20$ m (+ +). The numerically calculated volume flows presented in Table 3 are also included (o).

vorticity and energy), but can also be derived by assuming a pure geostrophic flow, yielding:

$$Q = 0.5 g' h_u^2 / f. \tag{17}$$

This transport rate may be compared with a slightly simplified version of eq. (16) obtained after the exponent is approximated with $\frac{1}{4}$. In this case, the following formula can be derived:

$$Q = 0.3(\theta f B^2 h_u / C_d)^{1/4} (g' h_u^2 / f)^{3/4}. \tag{18}$$

Fig. 8 illustrates the transport estimates given by eqs. (17) and (18). The latter formula suggests a considerable lower inflow rate than obtained by the former. For example, in the regime of observed inflows ($1 \times 10^4 - 2 \times 10^4$ m^3 s^{-1}) the flow rate given by eq. (17) is almost twice the calculated values obtained from the present model.

Note that when the flow is geostrophic and conserve potential vorticity and energy (in which case the flow become critical at some section in the channel) the flow is uniquely determined by the upstream conditions (cf. Whitehead et al., 1974). In the present model, the flow is subcritical and may be influenced by downstream conditions as well (which also can be the case when the flow is assumed to be geostrophic without using any other dynamical constraint). It appears, however, that this rarely occurs in the Bornholm Channel, since the downstream located Bornholm Basin is much deeper than the Arkona Basin, and the pycnocline (halocline) in the Bornholm Basin is in general located below the entrance depth of the Bornholm Channel.

5. Conclusions

A numerical two-layer model has been applied to the Bornholm Channel with the objective of studying the dynamics in the channel and to quantify the transport capacity using hydrographic conditions in the upstream Arkona Basin. The series of numerical calculations, where in particular the influence of rotation and bottom friction were investigated, indicate that each of these two terms are limiting the transport to a similar degree (to about 50% of the transport for the case excluding both terms), but that the combined effect leads to stronger reduction (30%) of the volume flow. The results rely on a simple parameterization of the bottom stress through a quadratic drag law. The exact choice of the drag coefficient, however, does not seem to be crucial for the transport capacity. The numerically calculated volume transports are in agreement with transport measurements performed in the Bornholm Channel.

An empirical formula, obtained from an analysis of the numerical results, relates the transport capacity in the Bornholm Channel to the density difference and pycnocline height in the Arkona Basin. The formula indicates that the channel transport is indeed lower than if calculated from a purely geostrophic flow. The formula may prove useful when applied to other channel-like constrictions governed by similar dynamical and topographical characteristics.

A final remark concerns the rather idealized channel topography used in the investigation. For a future study, it is suggested that the mathematical model should run with a grid based on the bottom topography taken from bathymetrical charts.

6. Acknowledgements

This work has been supported by the Swedish Natural Science Research Council (NFR). The authors are indebted to A. Omstedt, K. Borenäs and the two referees for suggestions and valuable support.

REFERENCES

Borenäs, K. and Lundberg, P. 1988. On the deep-water flow through the Faroe Bank Channel. *J. Geophys. Res. 93*, 1281–1292.

Chriss, T. M. and Caldwell, D. R. 1982. Evidence for the influence of form drag on bottom boundary layer flow. *J. Geophys. Res. 87*, 4148–4154.

Csanady, G. T. 1982. *Circulation in the coastal ocean.* Reidel Publishing Company, Dordrecht, 274 pp.

Fonselius, S. H. 1967. *Hydrography of the Baltic deep basins III.* Fishery Board of Sweden, Series Hydrography, Report No. 23, 1–97.

Funkquist, L., Gidhagen, L. and Svensson, U. 1987. The mathematical modelling of baroclinic waves and fronts in the ocean. *Appl. Math. Modelling 11*, 11–18.

Gill, A. E. 1976. Adjustment under gravity in a rotating channel. *J. Fluid Mech. 77*, 603–621.

Gill, A. E. 1977. The hydraulics of rotating-channel flow. *J. Fluid Mech. 80*, 641–671.

Grant, W. D., Williams, III, A. J. and Glenn, S. M. 1984. Bottom stress estimates and their prediction on the Northern California continental shelf during CODE-1: The importance of wave-current interaction. *J. Phys. Oceanogr. 14*, 506–527.

Jacobsen, T. S. 1980. *Sea water exchange of the Baltic, measurements and methods.* Belt Project, National Agency of Environment Protection, Denmark, 706 pp.

Lundberg, P. 1983. On the mechanics of the deep-water flow in the Bornholm Channel. *Tellus 35A*, 149–158.

Matthäus, W. 1984. Climatic and seasonal variability of oceanological parameters in the Baltic Sea. *Beitr. Meereskd. Heft 51*, 29–49.

Matthäus, W. 1985. Annual and long-term mean changes of salinity in the Arkona Basin. (In German.) *Beitr. Meereskd. Heft 53*, 17–26.

Omstedt, A. 1987. Watercooling in the entrance of the Baltic Sea. *Tellus 39A*, 254–265.

Omstedt, A. 1990. Modelling the Baltic Sea as thirteen sub-basins with vertical resolution. *Tellus 42A*, 286–301.

Pedersen, F. B. 1977. On dense bottom currents in the Baltic deep water. *Nordic Hydrology 8*, 297–316.

Petrén, O. and Walin, G. 1976. Some observations of the deep flow in the Bornholm strait during the period June 1973–December 1974. *Tellus 28*, 4–87.

Pingree, R. D. and Maddock, L. 1980. The effect of bottom friction and Earth's rotation on an island's wake. *J. Mar. Biol. Assoc. U.K. 60*, 99–508.

Pratt, L. J. 1986. Hydraulic control of sill flow with bottom friction. *J. Phys. Oceanogr. 16*, 1970–1980.

Spalding, D. B. 1981. A general-purpose computer program for multi-dimensional one- and two-phase flows. *J. Math. and Comput. in Simulation 23*, 267–276.

Spalding, D. B. and Markatos, N. C. 1983. *Computer simulation of multi-phase flows.* A course of 12 lectures. Rep. CFD/83/4, Imperial College, London.

Spalding, D. B. 1985. *The numerical computation of multi-phase flows.* Rep. CFD/85/7, Imperial College, London.

Stigebrandt, A. 1987. A model for the vertical circulation of the Baltic deep water. *J. Phys. Oceanogr. 17*, 1772–1785.

Walin, G. 1981. On the deep water flow into the Baltic. *Geophysica 17*, 75–93.

Whitham, G. B. 1974. *Linear and non-linear waves.* Wiley-Interscience, pp. 327.

Whitehead, J. A., Leetmaa, A. and Know, R. A. 1974. Rotating hydraulics of strait and sill flows. *Geophys. Fluid Dyn. 6*, 101–125.